LETTERS
nature photonics

Directional control of light by a nano-optical Yagi–Uda antenna

Terukazu Kosako, Yutaka Kadoya* and Holger F. Hofmann

The plasmon resonance of metal nanoparticles can direct light from optical emitters in much the same way that radiofrequency antennas direct the emission from electrical circuits. Recently, rapid progress has been made in the realization of single-element antennas for optical waves[1–12]. Because most of these devices are designed to optimize the local near-field coupling between the antenna and an emitter, the possibility of modifying the spatial radiation pattern has not yet received as much attention[13,14]. In the radiofrequency regime, a typical antenna design for high directivity is the Yagi–Uda antenna, which essentially consists of a one-dimensional array of antenna elements driven by a single feed element. By fabricating a corresponding array of nanoparticles, similar radiation patterns can be obtained in the optical regime[15–18]. Here, we present the experimental demonstration of directional control of radiation from a nano-optical Yagi–Uda antenna composed of appropriately tuned gold nanorods.

Directing the fluorescence from nanoscale emitters such as single molecules and single quantum dots is a key factor in a wide range of applications, from the efficient detection of molecules for biological diagnostics to photonic devices for quantum-information processing. It has long been known that the fluorescence of quantum emitters can be modified by controlling the optical resonances in the vicinity of the emitter[19]. Experimentally, the effect has been demonstrated using optical cavities composed of a pair of metallic[20] or dielectric mirrors[21] or photonic crystals[22]. In principle, the plasmon resonances of nanoparticles could achieve similar results on even smaller length scales[6,7,10–12,14], offering a promising alternative to cavity resonators for use in integrated nano-optical devices.

To develop the full potential of directional control by nanoparticles, we take our inspiration from radiofrequency (RF) technology, where Yagi–Uda antennas are known to achieve high directivities. Yagi–Uda antennas are composed of a linear array of metal rods working as feed, reflector and directors[23]. The electromagnetic wave emanating from the feed element induces currents in the other passive elements of the antenna array, resulting in phase-coherent emissions from all the elements in the array. Therefore, the Yagi–Uda antenna is a good candidate for directing the fluorescence from a nanoscale emitter placed on or near the feed element. The aim of this work is to demonstrate experimentally that a nano-optical Yagi–Uda antenna can be used to achieve directional radiation of light from the position of the feed element.

Figure 1 illustrates the typical geometry of a RF Yagi–Uda antenna. Because resonant elements cause reflections, the directors in front of the feed element are capacitively detuned to resonate at wavelengths shorter than the emitted wavelength λ. A single reflector element inductively detuned to wavelengths longer than λ is placed behind the feed to further reduce the radiation emitted in the backward direction. A high directivity can be obtained with distances of about 0.25λ between the feed and the reflector and about 0.3λ between the feed and the director and between the directors[16,23].

In the RF regime, antenna elements are realized by metal rods resonating at wavelengths of about twice their length. At optical frequencies, it is necessary to take into account the precise electromagnetic response of the metal as given by its complex dielectric constant. Specifically, the optical response is characterized by a negative real part that originates from the retardation of electron motion due to the electron mass. For sufficiently small particles, the kinetic energy of the electrons replaces the magnetic energy of the inductance in the electromagnetic response of the particle, resulting in a size-independent localized surface plasmon resonance determined by the shape and the dielectric constant of the particle.

In the case of nanorods, the resonance depends on the aspect ratios of the rod geometry, with elongated rods resonating at longer wavelengths than spherical particles, regardless of size. The essential properties of the nanorods can be summarized in terms of their volume V, a shape-dependent depolarization factor N (ref. 24), and the dielectric constant ϵ_r of the rod material relative to the surrounding medium ($\epsilon_r = \epsilon_{\text{rod}}/\epsilon_{\text{med}}$). For a given wavelength λ, the polarizability α is then given by[16]

$$\alpha = \frac{V}{(1/(\epsilon_r - 1)) + N - i(4\pi^2 V/3\lambda^3)} \tag{1}$$

The dipole resonance is capacitively (inductively) detuned for $N > |\text{Re}[1/(\epsilon_r - 1)]|$ $(N < |\text{Re}[1/(\epsilon_r - 1)]|)$. The value of N can be adjusted by selecting the appropriate aspect ratio of the nanorods. For practical purposes, it is convenient to keep the cross-section of the nanorods constant while varying only their length. Thus, the relation between the detuning and the length of the nanorods

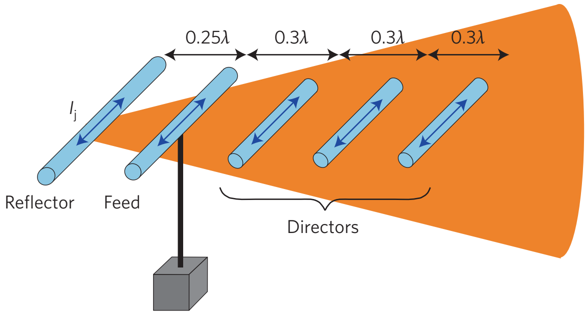

Figure 1 | Typical geometry of a five-element RF Yagi–Uda antenna. Directional emission is obtained through the passive response of reflector and director to the actively driven feed. To obtain the same mechanism of directional control at visible wavelengths it is necessary to find a way to recreate the conditions required for various elements to act as reflector, feed and director elements. We can exploit the dependence of the resonant frequency of metallic nanoparticles on their spatial dimensions for this purpose.

Graduate School of Advanced Sciences of Matter, Hiroshima University, Kagamiyama 1-3-1, Higashihiroshima 739-8530, Japan. *e-mail: kd@hiroshima-u.ac.jp

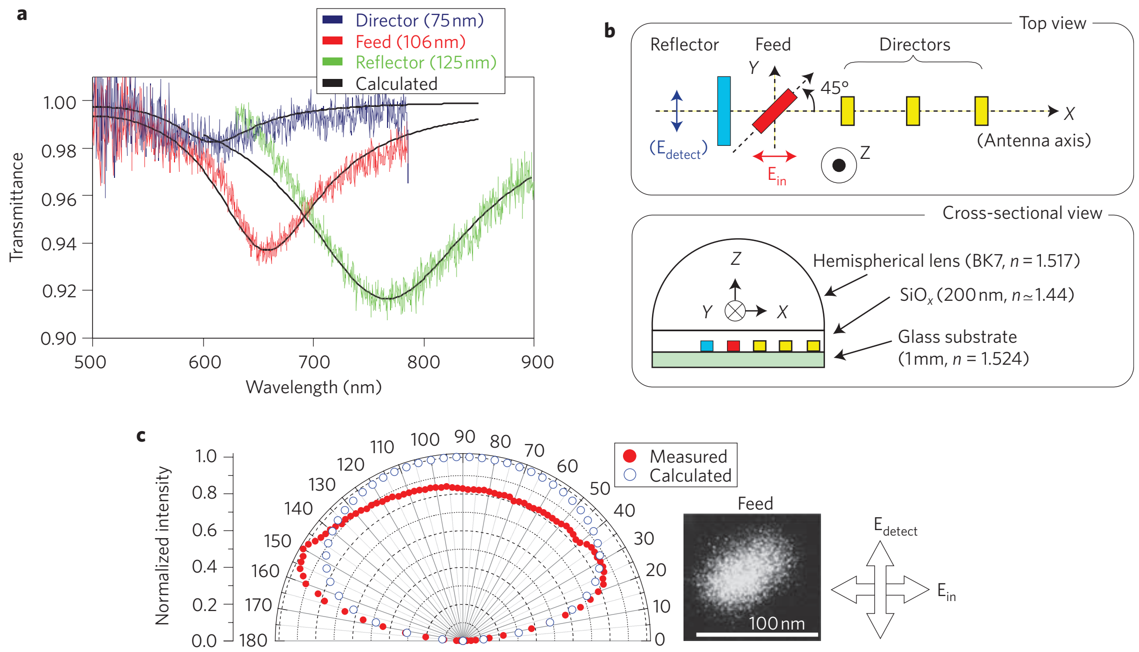

Figure 2 | Properties of the antenna elements and the measurement set-up. a, Transmission spectra for the three different nanorod geometries used in the antenna array. The black solid lines are the results of the fitting using equation (1). **b**, Top view of the antenna layout and the cross-sectional illustration of the set-up for measuring the emission pattern. **c**, Emission pattern of a feed element. The solid and open circles represent the experimental results and the theoretical prediction, respectively. The inset shows the SEM image of the feed element.

appears to be the same as in the RF regime, with shorter (longer) rods having shorter (longer) wavelength resonances.

In addition to the negative real part of the dielectric constant, it is also necessary to consider its imaginary part, which describes the absorption of radiation energy in the material. For antenna elements, it is essential that the losses due to absorption are sufficiently smaller than the emission of radiation into the far field. As we discussed in our previous work, radiative losses contribute the volume-dependent term in the denominator of the polarization given by equation (1), and the material losses contribute the volume-independent term originating from the imaginary part of the dielectric constant. Specifically, the ratio of material losses and radiative losses is[16]

$$\gamma = \frac{3\lambda^3}{4\pi^2 V}\frac{\mathrm{Im}[\epsilon_r]}{|\epsilon_r - 1|^2} \qquad (2)$$

This relation shows that thermal losses can be reduced by increasing the size of the nanoparticles used in the antenna array.

For the experiment, antenna arrays made of 50-nm-thick gold nanorods were fabricated lithographically on a glass substrate. The antennas were then embedded in a sputter-deposited SiO_x film to suppress the effects of a varying index of refractivity on the coupling between array elements. The resonant wavelength of the different nanorod geometries was confirmed experimentally by measurements of the transmission spectra of light polarized parallel to the major axis of the nanorods. Figure 2a shows the transmission spectra for the three different nanorod geometries used in the antenna arrays. The resonance wavelengths were found to be ~610 nm, 655 nm, and 770 nm for nanorods of length 75 nm (director), 106 nm (feed) and 125 nm (reflector), respectively. The reflector is therefore inductively detuned and the directors are capacitively detuned when the antenna is operating at a wavelength near the feed resonance.

The thermal losses of the antenna elements can be determined by obtaining the effective volume V and the depolarization factor N from a fit of the observed transmission spectra with the imaginary part of the polarizability given by equation (1). The black lines in Fig. 2a show the results of fitting using the reported dielectric constant of gold[25]. Using the corresponding values of V in equation (2), we find that the ratios of material losses and radiative losses at the operating wavelength of 662 nm used in the following antenna measurements are 0.38, 0.285 and 0.438 for the feed, reflector and director, respectively. Therefore, the thermal losses in the material are below half of the radiated energy in all of the elements, indicating that more than two-thirds of the total input energy is re-emitted. Assuming that the interference effects between the emissions of the elements average out when integrated over all directions, we can therefore expect that the complete antenna arrays also emit more than two-thirds of the energy supplied to the feed into the far field.

For the purpose of emulating the local emission from an emitter arranged at the feed point, we used the polarization dependence of the nanorod response to an external driving field. The feed element was tilted by 45° towards the antenna axis, as shown in the top view illustration in Fig. 2b, and driven by the light polarized parallel to the antenna axis (X). Owing to its diagonal alignment, the feed element converts a part of the driving light into light polarized along the major axis of the passive elements (Y). As we confirmed in a separate test measurement, the passive elements emit only a negligibly small amount of light polarized perpendicular to the driving field. We can therefore conclude that almost all of the Y-polarized light originates from the plasma oscillations of the feed element. Thus, the emission patterns obtained by detecting only the Y-polarization correspond to the emission patterns of radiation from just the feed element, modified by the passive response of the other antenna elements.

In the measurement of the radiation pattern, the sample was set on a prism, and covered by a hemispherical lens with index-matching oil to avoid refraction and total reflection, as shown in the cross-sectional diagram in Fig. 2b. The feed element was driven by a laser diode at a wavelength of 662 nm through a polarizer, and the emission was detected in the X–Z plane, which is orthogonal to the substrate and includes the antenna axis, with a photodiode through another polarizer.

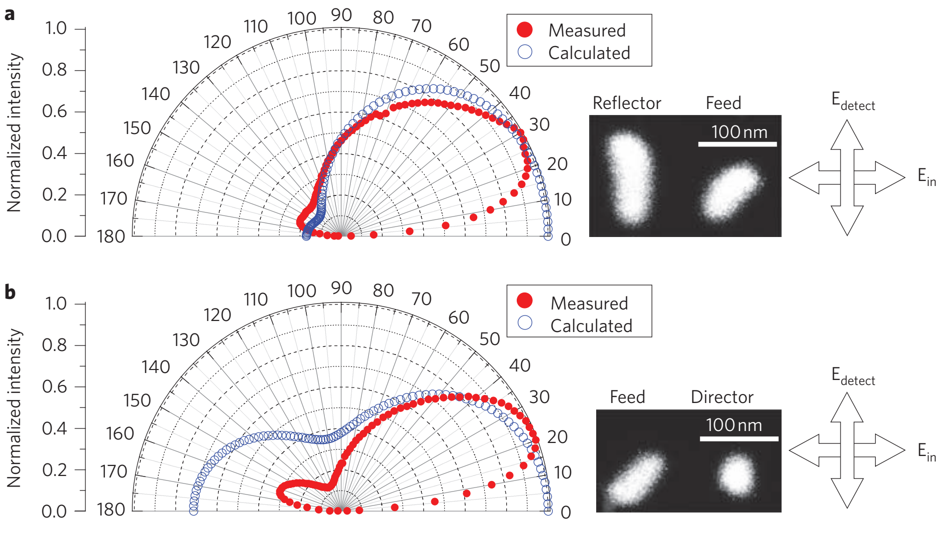

Figure 3 | Radiation patterns of two-element antennas. The insets show the SEM images of the antennas. The experimental results and the theoretical predictions are plotted with solid and open circles, respectively. **a**, Feed–reflector antenna. **b**, Feed–director antenna.

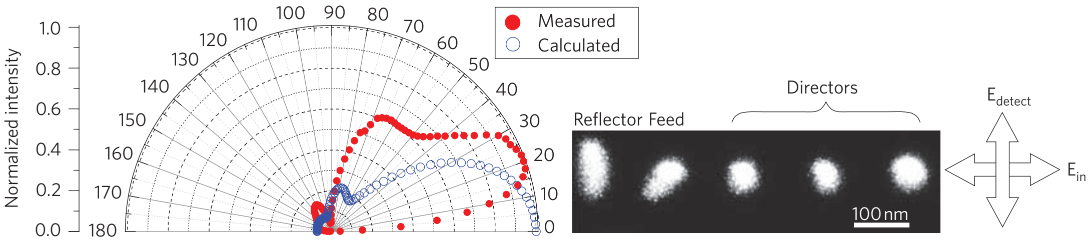

Figure 4 | Measured (solid circles) and predicted (open circles) radiation patterns of the five-element Yagi–Uda antenna. The inset shows the SEM image of the antenna.

Figure 2c shows the emission pattern of a feed element without any reflectors or directors. The emission is nearly symmetric around the normal to the surface, as expected for emission from a single dipole. The slight asymmetry of the pattern is probably caused by a small misalignment between the centre of the spherical lens and the antenna elements. Most significantly, the intensity rapidly diminishes for angles below 20° and above 160°. This effect indicates a small mismatch of the indices of refractivity above and below the dipole. The angular dependence is consistent with that predicted for a ratio of about $1.52/1.44 = 1.06$, corresponding to the indices of refractivity of the substrate and the SiO_x layer, as shown by the open circles in the figure.

To confirm that the reflector and director elements have the desired effect on the directionality of the emission, we fabricated antennas composed of only two elements, the feed and either a reflector or a director with a spacing of 125 nm (0.27λ) between the elements. Figure 3a shows the measured emission pattern of the feed–reflector antenna (solid dots). Clearly, the presence of the reflector behind the feed strongly suppresses the backward emission. However, the angle of emission is still rather wide. Note that the observed pattern is in good agreement with the prediction (open circles) based on the coupled point dipole model[16], except for the influence of index mismatching mentioned above.

Shown in Fig. 3b by the red solid dots is the measured emission pattern of the feed–director antenna. The spacing between the elements is the same as that for the feed–reflector antenna. However, the passive element is now a capacitively detuned director in front of the feed. The result thus illustrates how the capacitive detuning of the director enhances emission in the direction of the passive antenna element. The angle of emission in the forward direction is even somewhat narrower than that of the feed–reflector antenna. In fact, the experimental result shows a stronger directivity than that expected from the dipole model[16] (open circles). The discrepancy may arise from the failure of the dipole approximation due to the proximity or shape of the elements. In particular, the tilt of the feed element means that the edge of the feed gets very close to the director, which may cause a significant contribution of higher-order multipole moments to the coupling.

The results for a complete five-element Yagi–Uda antenna are shown in Fig. 4. As can be seen in the scanning electron microscopy (SEM) image in the inset, this antenna array consists of a feed, a reflector and three directors. The distance between the feed and the reflector is 125 nm, as before, whereas that between the feed and the director and that between the directors have been changed to 150 nm to correspond to the choice of parameters from our previous theoretical study[16]. The radiation pattern obtained from this antenna array shows a directionality with the emission concentrated around angles close to the region around 0–20°, where the small mismatch of the index of refractivity suppresses the emission. Taking into account this suppression of a significant part of the forward emission, we observe fairly good qualitative agreement between the experimental results (red solid dots) and the theoretical prediction from the dipole model (circles). In particular, the experimental data clearly shows a side lobe around 70° and a small backward emission separated by a minimum at 110°. These features of the emission pattern originate from the characteristic interferences between radiation from different array elements, indicating that the directionality of the emission is indeed obtained from the coupling of the array elements.

In conclusion, we have experimentally demonstrated the realization of a nano-optical Yagi–Uda antenna composed of an array of appropriately tuned gold nanorods. Our results clearly show that the basic principles of RF antenna design can be applied successfully to obtain the same kind of directivity in the optical regime. It should therefore be possible to guide the emission of light from a nanoscale emitter using metallic structures with a total size that is not much larger than a single wavelength. As the results for two element antennas show, even very simple arrangements can significantly improve the directionality of emission. Thus, nano-optical antenna arrays have the potential of becoming a highly flexible and useful component of future nano-optical technologies.

Received 11 January 2010; accepted 8 February 2010;

References

1. Crozier, K. B., Sundaramurthy, A., Kino, G. S. & Quate, C. F. Optical antennas: resonators for local field enhancement. *J. Appl. Phys.* **94,** 4632–4642 (2003).
2. Fromm, D. P., Sundaramurthy, A., Schuck, P. J., Kino, G. & Moerner, W. E. Gap-dependent optical coupling of single 'bowtie' nanoantennas resonant in the visible. *Nano Lett.* **4,** 957–961 (2004).
3. Schuck, P. J., Fromm, D. P., Sundaramurthy, A., Kino, G. S. & Moerner, W. E. Improving the mismatch between light and nanoscale objects with gold bowtie nanoantennas. *Phys. Rev. Lett.* **94,** 017402 (2005).
4. Mühlschlegel, P., Eisler, H.-J., Martin, O. J. F., Hecht, B. & Pohl, D. W. Resonant optical antennas. *Science* **308,** 1607–1609 (2005).
5. Aizpurua, J. *et al.* Optical properties of coupled metallic nanorods for field-enhanced spectroscopy. *Phys. Rev. B* **71,** 235420 (2005).
6. Farahani, J. N., Pohl, D. W., Eisler, H.-J. & Hecht, B. Single quantum dot coupled to a scanning optical antenna: a tunable superemitter. *Phys. Rev. Lett.* **95,** 017402 (2005).
7. Kühn, S., Håkanson, U., Rogobete, L. & Sandoghdar, V. Enhancement of single-molecule fluorescence using a gold nanoparticle as an optical nanoantenna. *Phys. Rev. Lett.* **97,** 017402 (2006).
8. Sundaramurthy, A. *et al.* Toward nanometer-scale optical photolithography: utilizing the near-field of bowtie optical nanoantennas. *Nano Lett.* **6,** 355–360 (2006).
9. Fromm, D. P. *et al.* Exploring the chemical enhancement for surface-enhanced Raman scattering with Au bowtie nanoantennas. *J. Chem. Phys.* **124,** 061101 (2006).
10. Muskens, O. L., Giannini, V., Sánchez-Gil, J. A. & Rivas, J. G. Strong enhancement of the radiative decay rate of emitters by single plasmonic nanoantennas. *Nano Lett.* **7,** 2871–2875 (2007).
11. Bakker, R. M. *et al.* Enhanced localized fluorescence in plasmonic nanoantennae. *Appl. Phys. Lett.* **92,** 043101 (2008).
12. Bakker, R. M. *et al.* Nanoantenna array-induced fluorescence enhancement and reduced lifetimes. *New J. Phys.* **10,** 125022 (2008).
13. Taminiau, T. H., Moerland, R. J., Segerink, F. B., Kuipers, L. & van Hulst, N. F. $\lambda/4$ Resonance of an optical monopole antenna probed by single molecule fluorescence. *Nano Lett.* **7,** 28–33 (2007).
14. Taminiau, T. H. *et al.* Optical antennas direct single-molecule emission. *Nature Photon.* **2,** 234–237 (2008).
15. Li, J., Salandrino, A. & Engheta, N. Shaping light beams in the nanometer scale: A Yagi–Uda nanoantenna in the optical domain. *Phys. Rev. B* **76,** 245403 (2007).
16. Hofmann, H. F., Kosako, T. & Kadoya, Y. Design parameters for a nano-optical Yagi–Uda antenna. *New J. Phys.* **9,** 217 (2007).
17. Pellegrini, G., Mattei, G., Mazzoldi, P. Tunable, directional and wavelength selective plasmonic nanoantenna arrays. *Nanotechnology*, **20,** 065201 (2009).
18. Koenderink, A. F. Plasmon nanoparticle array waveguides for single photon and single plasmon sources. *Nano Lett.* **9,** 4228–4233 (2009).
19. Purcell, E. M. Spontaneous emission probabilities at radio frequencies. *Phys. Rev.* **69,** 681 (1946).
20. Hulet, R. G., Hilfer, E. S. & Kleppner, D. Inhibited spontaneous emission by a Rydberg atom. *Phys. Rev. Lett.* **55,** 2137–2140 (1985).
21. Björk, G., Machida, S., Yamamoto, Y. & Igeta, K. Modification of spontaneous emission rate in planar dielectric microcavity structures. *Phys. Rev. A* **44,** 669–681 (1991).
22. Ogawa, S., Imada, M., Yoshimoto, S., Okano, M. & Noda, S. Control of light emission by 3D photonic crystals. *Science* **305,** 227–229 (2004).
23. Balanis, C. A. *Antenna Theory Analysys and Design* 3rd edn, 577 (John Wiley & Sons, 2005).
24. Craig, F. B. & Donald, R. H. *Absorption and Scattering of Light by Small Particles* (Wiley-VCH, 2004).
25. Johnson, P. B. & Christy, R. W. Optical constants of the noble metals. *Phys. Rev. B* **6,** 4370–4379 (1972).

Acknowledgements

Part of this work was supported by the Grant-in-Aid Scientific Research from the Japan Society for the Promotion of Science.

Author contributions

All authors conceived and designed the experiment. T.K. prepared the samples and carried out the measurement. All authors participated in the analysis of the data and in the writing of the paper.

Additional information

The authors declare no competing financial interests. Reprints and permission information is available online at http://npg.nature.com/reprintsandpermissions/. Correspondence and requests for materials should be addressed to Y.K.